University of Nebraska - Lincoln

DigitalCommons@University of Nebraska - Lincoln

Papers in Natural Resources

Natural Resources, School of

2006

Relationship between gross primary production and chlorophyll content in crops: Implications for the synoptic monitoring of vegetation productivity

Anatoly A. Gitelson
University of Nebraska at Lincoln, agitelson2@unl.edu

Andrés Viña
University of Nebraska - Lincoln

Shashi Verma
University of Nebraska - Lincoln, sverma1@unl.edu

Donald C. Rundquist
University of Nebraska - Lincoln, drundquist1@unl.edu

Timothy J. Arkebauer
University of Nebraska - Lincoln, tarkebauer1@unl.edu

See next page for additional authors

Follow this and additional works at: https://digitalcommons.unl.edu/natrespapers

Part of the Natural Resources and Conservation Commons

Authors

Anatoly A. Gitelson, Andrés Viña, Shashi Verma, Donald C. Rundquist, Timothy J. Arkebauer, Galina P. Keydan, Bryan Leavitt, Veronica Ciganda, George G. Burba, and Andrew E. Suyker

Relationship between gross primary production and chlorophyll content in crops: Implications for the synoptic monitoring of vegetation productivity

Anatoly A. Gitelson,[1,2] Andrés Viña,[1,3] Shashi B. Verma,[2] Donald C. Rundquist,[1,2] Timothy J. Arkebauer,[4] Galina Keydan,[1] Bryan Leavitt,[1] Veronica Ciganda,[1,4] George G. Burba,[2,5] and Andrew E. Suyker[2]

[1] Accurate estimation of spatially distributed CO_2 fluxes is of great importance for regional and global studies of carbon balance. We applied a recently developed technique for remote estimation of crop chlorophyll content to assess gross primary production (GPP). The technique is based on reflectance in two spectral channels: the near-infrared and either the green or the red-edge. We have found that in irrigated and rainfed crops (maize and soybean), midday GPP is closely related to total crop chlorophyll content. The technique provided accurate estimations of midday GPP in both crops under rainfed and irrigated conditions with root mean square error of GPP estimation of less than 0.3 mg CO_2/m^2s in maize (GPP ranged from 0 to 3.1 mg CO_2/m^2s) and less than 0.2 mg CO_2/m^2s in soybean (GPP ranged from 0 to 1.8 mg CO_2/m^2s). Validation using an independent data set for irrigated and rainfed maize showed robustness of the technique; RMSE of GPP prediction was less than 0.27 mg CO_2/m^2s.

1. Introduction

[2] The importance of studying vegetation dynamics has been recognized for decades [e.g., *Box*, 1978; *Lieth*, 1975]. A key driver has been the interest in understanding the patterns of terrestrial vegetation productivity and its relationships with global biogeochemical cycles of carbon and nitrogen [*Cao and Woodward*, 1998; *Dixon et al.*, 1994; *Lieth*, 1975; *Myneni et al.*, 1997, 2001; *Schimel*, 1998]. Vegetation productivity is the basis of all the biospheric functions on the land surface (excluding the very small contribution by chemosynthetic autotrophic organisms), and is simply defined as the production of organic matter through photosynthesis. The total amount of organic matter produced through photosynthesis is termed gross photosynthesis, and if expressed as the integral of the organic matter produced by all the individual plants in a defined area per unit of time, is termed gross primary productivity (GPP).

[3] The vegetation productivity has been assessed through the use of micrometeorological approaches, by means of studying whole-community gas exchange [e.g., *Verma*, 1990]. Micrometeorological methods measure the entire net carbon flux between the land surface and the atmosphere, or what is called net ecosystem carbon dioxide exchange (NEE). Many field studies in different ecosystems across the globe have used tower-based eddy covariance techniques to provide information on seasonal dynamics and interannual variation of NEE [e.g., *Baldocchi*, 2003, and references therein; *Flanagan et al.*, 2002; *Suyker et al.*, 2003; *Verma et al.*, 2005].

[4] Numerous studies have estimated GPP and daytime ecosystem respiration (R_e) from NEE data [e.g., *Biscoe et al.*, 1975; *Falge et al.*, 2002; *Gilmanov et al.*, 2003; *Suyker et al.*, 2005; *Turner et al.*, 2003]. Measurements of NEE were used to calculate GPP as (GPP = 0 during night):

$$GPP = NEE - R_e \qquad (1)$$

where CO_2 uptake is positive and CO_2 release is negative. Daytime R_e is estimated by adjusting nighttime NEE to daytime temperature [e.g., *Falge et al.*, 2002]. However, the NEE and GPP data are representative of only a small footprint area, and scaling up beyond the footprint to an entire region is challenging [*Wofsy and Harriss*, 2002].

---

[1]Center for Advanced Land Management Information Technologies, University of Nebraska, Lincoln, Nebraska, USA.

[2]School of Natural Resources, University of Nebraska, Lincoln, Nebraska, USA.

[3]Now at Center for Systems Integration and Sustainability, Department of Fisheries and Wildlife, Michigan State University, East Lansing, Michigan, USA.

[4]Department of Agronomy and Horticulture, University of Nebraska, Lincoln, Nebraska, USA.

[5]Now at LI-COR Biosciences, Inc., Environmental Division, Lincoln, Nebraska, USA.

[5] Remote sensing is the technology by which the electromagnetic energy emitted or reflected by the Earth's surface is recorded by sensors on the ground, aircraft and spacecraft. The synoptic view provided by imaging sensors makes remote sensing an attractive and powerful tool for studying vegetation productivity, at scales ranging from local to global. Given that vegetation productivity is directly related to the interaction of solar radiation with the plant canopy [*Knipling*, 1970], remote sensing techniques can be used to measure vegetation productivity. Since December 1999 the U.S. National Aeronautics and Space Administration (NASA) Earth Observing System (EOS) produces a regular global estimate of net primary production (NPP) for the entire globe [e.g., *Running et al.*, 2000, 2004]. This estimate is based on the original logic of *Monteith* [1972, 1977], who suggested that the GPP of stress-free (i.e., well watered and fertilized) annual crops, was linearly related to the amount of photosynthetically active radiation they absorbed, following the expression:

$$GPP \propto \varepsilon \times \Sigma APAR \qquad (2)$$

Where $\Sigma APAR$ is absorbed photosynthetically active radiation integrated over a time period, and ε is light use efficiency (LUE) or the efficiency of the conversion of absorbed light into aboveground biomass. Several studies [*Asrar et al.*, 1992; *Sellers*, 1985, 1987; *Sellers et al.*, 1992] found that under specified canopy reflectance properties, APAR can be estimated remotely, using the Normalized Difference Vegetation Index (NDVI, the difference between reflectance (R) in the near-infrared (NIR) and red spectral regions, normalized by their sum: $(R_{NIR} - R_{red})/(R_{NIR} + R_{red})$), through the expression:

$$fAPAR = APAR/PAR \propto NDVI \qquad (3)$$

Where PAR is the incident photosynthetically active radiation and fAPAR is the fraction of PAR absorbed by the vegetation. *Ruimy et al.* [1994] underscored the fact that the linear relationship between fAPAR and NDVI is an approximation, and it is only valid during the growing stage. In fact, a comparison of models revealed that the NDVI-derived APAR is significantly lower than an independently modeled APAR by a consistent global discrepancy of 28% [*Ruimy et al.*, 1999]. A likely explanation for this is that a significant decrease in the sensitivity of NDVI is observed when fAPAR exceeds 0.7 [*Asrar et al.*, 1984, 1992; *Goward and Huemmrich*, 1992; *Roujean and Breon*, 1995; *Walter-Shea et al.*, 1997; *Viña and Gitelson*, 2005]. Therefore one of the main problems of the remote assessment of GPP is caused by the uncertainty of the NDVI/fAPAR relationship, which is normally assumed to be linear [e.g., *Running et al.*, 2000].

[6] Although photosynthetic rates have been shown to respond linearly to APAR in annual crops, curvilinear relationships have been observed in other vegetation types [*Ruimy et al.*, 1995; *Turner et al.*, 2003]. Nevertheless, near-linear relationships can be forced, if the time interval is extended [*Ruimy et al.*, 1995]. According to *Monteith* [1972], LUE is a relatively conservative value among plant formations of the same metabolic type. However, it can vary with phenological stage, climatic condition, temperature,

and water stress [e.g., *Jarvis and Leverenz*, 1983]. Therefore the uncertainty of the estimation of terrestrial GPP with Monteith's logic might be considerable, when no information about factors influencing LUE is introduced.

[7] *Running et al.* [2000] used biome-constant values of LUE in the BIOME-BGC model to produce the NASA-EOS Global NPP product, and LUE variability was parameterized by the use of a look-up table that integrates biome-specific edaphic and climatic characteristics. These values of LUE were then modified with functions driven by surface temperature and vapor pressure deficit obtained from coarse resolution satellite-based weather data [*Running et al.*, 2004]. Other studies have shown that LUE variability is species-specific rather than biome-specific [e.g., *Ahl et al.*, 2004], which further complicates the parameterization of LUE in regional to global models of GPP and NPP.

[8] *Rahman et al.* [2004] suggested that to accurately estimate CO_2 fluxes of terrestrial vegetation it is necessary to take into account the changes in LUE. They produced a "continuous field" LUE retrieved from satellite data, using the photochemical reflectance index (PRI) as a proxy of LUE [e.g., *Gamon et al.*, 1992], without referring to look-up tables or predetermined biome/community-specific LUE values. PRI is defined as:

$$PRI = (R_{531} - R_{570})/(R_{531} + R_{570}) \qquad (4)$$

Where R_{531} and R_{570} are reflectances at 531 nm 570 nm, respectively. Several studies have shown the linear relationship between PRI and LUE in different vegetation types [e.g., *Nichol et al.*, 2000, 2002]. However, *Barton and North* [2001] showed that PRI was most sensitive to changes in leaf area index (LAI), and concluded that the potential use of this index to predict LUE will require an independent estimate of LAI.

[9] While the above mentioned approaches provide ways for the synoptic estimation of vegetation productivity in different ecosystems, an accurate synoptic estimation is still elusive. Thus new approaches are needed. In this study, we propose a new remote technique to estimate midday GPP in crops that builds upon Monteith's logic. However, it does not depend on the NDVI/fAPAR linearity assumption, and it does not depend on the constancy, preestablished variability or biome/species specificity of LUE. The approach is based on the remote estimation of crop chlorophyll content (Chl). Since long- or medium-term changes in canopy Chl are related to crop phenology, canopy stresses and photosynthetic capacity of the vegetation [e.g., *Ustin et al.*, 1998; *Zarco-Tejada et al.*, 2002], it can also be related to GPP. It was found that canopy level Chl may appear to be the community property most relevant for the prediction of productivity [*Whittaker and Marks*, 1975; *Dawson et al.*, 2003]. The specific objectives of this study were: (1) to evaluate existing remote sensing techniques for the estimation of GPP (retrieved from measured NEE through a tower-based eddy covariance technique) in irrigated and rainfed maize and soybean; (2) to establish the relationship between GPP and crop Chl in maize and soybean; and (3) to test the accuracy and robustness of a remote sensing technique, developed for canopy Chl retrieval, in the remote estimation of GPP in crops. We concentrated our efforts in the remote estimation of GPP in crops, because they are the most

Table 1. Crops and Their Management in Sites 1, 2 and 3 in 2001, 2002, and 2003

Years	2001	2002	2003
Site 1	irrigated maize	irrigated maize	irrigated maize
Site 2	irrigated maize	irrigated soybean	irrigated maize
Site 3	rainfed maize	rainfed soybean	rainfed maize

pervasive anthropogenic biome. Relatively simple in vegetation structure, crops play an important role in the global cycles of carbon, water, and nutrients as well as influencing local and regional weather.

2. Methods

[10] The study sites are located at the University of Nebraska-Lincoln Agricultural Research and Development Center near Mead, Nebraska, U.S.A. The first two sites (here denoted as sites 1 and 2, respectively) are 65-ha fields equipped with center pivot irrigation systems. The third site (denoted as site 3) is of approximately the same size, but relies entirely on rainfall. All three sites were uniformly tilled prior to the initiation of the research program. Since the initiation of the study, all sites have been under no till. Site 1 is under continuous maize, while sites 2 and 3 are under maize-soybean rotation (Table 1). Prior to initiation of the study, the irrigated sites (1 and 2) had a 10-year history of maize-soybean rotation under no till. The rainfed site (3) had a variable cropping history of primarily wheat, soybean, oats, and maize grown in 2 to 4 ha plots with tillage.

2.1. CO$_2$ Flux

[11] Micrometeorological eddy covariance data collection began on 25 May 2001 at sites 1 and 2, and on 13 June 2001, at site 3. To have sufficient upwind fetch (in all directions), eddy covariance sensors were mounted at 3 m above the ground while the canopy was shorter than 1 m, and later moved to a height of 6.2 m until harvest (details are given by *Suyker et al.* [2004]). The study sites represented approximately 90–95% of the flux footprint during daytime and 70–90% during nighttime [e.g., *Schuepp et al.*, 1990]. Daily midday NEE values were computed by integrating the CO$_2$ fluxes collected by the eddy covariance tower from 1000 to 1500 LT.

[12] Eddy covariance measurements of fluxes of CO$_2$, water vapor, sensible heat, and momentum were made using the following sensors: an omnidirectional 3-D sonic anemometer (Model R3: Gill Instruments Ltd., Lymington, UK), a closed path infrared CO$_2$/H$_2$O gas analyzing system (Model LI6262: LI-COR Inc., Lincoln, Nebraska), and an open-path infrared CO$_2$/H$_2$O gas analyzing system (Model LI7500: LI-COR Inc., Lincoln, Nebraska). Hourly averaged fluxes were calculated. Fluxes were corrected for inadequate sensor frequency response (*Moore* [1986], *Massman* [1991], *Suyker and Verma* [1993], in conjunction with cospectra calculated from this study), and adjusted for the variation in air density due to the transfer of water vapor [e.g., *Webb et al.*, 1980]. More details of the measurements and calculations are given elsewhere [*Suyker et al.*, 2004].

[13] Daytime estimates of R_e were obtained from the night CO$_2$ exchange temperature relationship [e.g., *Falge*

et al., 2002; *Xu and Baldocchi*, 2003]. To minimize problems related to insufficient turbulent mixing at night, following an analysis similar to *Barford et al.* [2001], we selected a threshold mean wind speed (U) of 2.5 m s^{-1} (corresponding to a friction velocity, u_* of 0.25 m s^{-1}, approximately). For $U < 2.5$ m s^{-1}, data were filled in using biweekly CO$_2$ exchange temperature relationships from windier conditions. The midday GPP (in mg CO$_2$/m^{2}s, hereafter mg/m^{2}s) was then obtained by subtracting midday R_e (from 1000 to 1500 LT) from midday NEE as in equation (1).

2.2. Leaf Area Index

[14] Within each site, six small (20 m $\times$ 20 m) plot areas were established for detailed process level studies. Six locations per site were selected using fuzzy k-means clustering [*Minasny and McBratney*, 2003] applied to seven layers of previously collected, spatially dense information (elevation, soil type, electric conductivity, soil organic matter content, digital aerial photography and 4 years of yield map data). The resulting intensive measurement zones (IMZs) represent all major occurrences of soil and crop production zones within each site.

[15] Plant populations were determined for each IMZ. On each sampling date, plants from a 1 m length of either of two rows within each IMZ were collected and the total number of plants recorded. Collection rows were alternated on successive dates to minimize edge effects on subsequent plant growth. Plants were transported on ice to the laboratory. In the lab, plants were dissected into green leaves, dead leaves, stems, and reproductive organs. The leaves were processed through an area meter (Model LI-3100, LI-COR, Inc., Lincoln, Nebraska) and the leaf area per plant was determined. For each IMZ, the total and green leaf area per plant was multiplied by the plant population (number of plants/m^2) to obtain total and Green LAI. The data at the six IMZs were area-weighted averaged to obtain a site-level value. Standard deviations of the destructive sampling of LAI ranged from 0.05 m^2/m^2 at the beginning of the growing season (day of the year (DOY) 163) to 0.48 m^2/m^2 before the peak of maximum LAI (around DOY 180).

2.3. Absorbed PAR

[16] Daily measurements of fAPAR were obtained using the following procedure: Incoming PAR (PAR$_{inc}$) was measured with point quantum sensors (LI-190, LI-COR Inc., Lincoln, Nebraska) pointing to the sky, and placed 6 m above the surface. PAR reflected by the canopy and soil (PAR$_{out}$) was measured with point quantum sensors pointing downward, and placed 6 m above the ground. PAR transmitted through the canopy (PAR$_{tran}$) was measured with line quantum sensors (LI-191, LI-COR Inc., Lincoln, Nebraska) placed at about 2 cm above the ground, looking upward; and PAR reflected by the soil (PAR$_{soil}$) was measured with line quantum sensors placed about 12 cm above the ground, looking downward. Absorbed PAR (APAR) was calculated as [*Goward and Huemmrich*, 1992]:

$$\text{APAR} = \text{PAR}_{inc} - \text{PAR}_{out} - \text{PAR}_{trans} + \text{PAR}_{soil} \quad (5)$$

The fractional absorbed PAR (fAPAR) was calculated as APAR/PAR$_{inc}$.

2.4. Leaf Chl Content

[17] Biweekly spectral reflectance measurements (in the range 400 to 900 nm) of upper canopy leaves (Chl$_{upper}$) were carried out in situ using an Ocean Optics USB2000 radiometer, equipped with a leaf clip (details given by *Viña et al.* [2004] and *Gitelson et al.* [2005]). Total leaf chlorophyll content was retrieved from reflectance spectra using a nondestructive technique [*Gitelson et al.*, 2003a]. Reflectance in the red edge spectral band between 700 and 720 nm and in the NIR between 760 and 800 nm, were used in the model Chl = $a \times [(R_{NIR}/R_{red\ edge}) - 1]$ [*Gitelson et al.*, 2003a]. To calibrate the model, total leaf Chl content was measured analytically in the lab and the coefficient a was determined. For both species in the range of total Chl from 2.44 through 918 mg/m^2, coefficient a was 330.6 mg/m^2, and a coefficient of determination (r^2) of the linear relationship between Chl and the model $[(R_{NIR}/R_{red\ edge}) - 1]$ was 0.95. Root Mean Square Error (RMSE) of leaf Chl retrieval from reflectance measurements in both species was less than 60 mg/m^2.

2.5. Total Canopy Chl Content

[18] Total Chl in the canopy was estimated as Chl$_{est}$ = Chl$_{upper}$ × (green LAI), where Chl$_{upper}$ is leaf Chl content in upper canopy leaves. To test whether Chl$_{upper}$ is representative of the entire canopy Chl, we compared Chl$_{est}$ with measured total Chl content in the canopy (Chl$_{meas}$). To find Chl$_{meas}$, Chl content of all leaves (Chl$_i^{leaf}$) of 22 maize and 14 soybean plants were retrieved from reflectance measurements using the nondestructive technique described earlier. Areas of each of these leaves (S$_i^{leaf}$) were measured with an area meter (Model LI-3100A, LI-COR, Inc., Lincoln, Nebraska). Total Chl in the entire plant, expressed as the amount of Chl per unit of ground S$_g$ (i.e., g/m^2) was calculated as Chl$_{meas}$ = $\Sigma_{i=1}^{n}$ (Chl$_i^{leaf}$ × S$_i^{leaf}$)/S$_g$, where n is total number of leaves in each plant. The measured and estimated (by the model $[(R_{NIR}/R_{red\ edge}) - 1]$) total Chl in the canopy were closely related: the RMSE of Chl estimation was 0.31 g/m^2 for maize (in the range of Chl from 0.03 to 4.33 g/m^2) and 0.15 g/m^2 (Chl ranged from 0.02 to 2.15 g/m^2) for soybean. This suggests that total Chl in the canopy can be accurately estimated using the product of green LAI and Chl in upper canopy leaves [*Gitelson et al.*, 2005].

2.6. Crop Reflectance

[19] Spectral measurements at the canopy/community level were made using hyperspectral radiometers mounted on "Goliath," an all-terrain sensor platform [*Rundquist et al.*, 2004]. A dual-fiber optic system, with two intercalibrated Ocean Optics USB2000 radiometers, was used to collect radiometric data in the range 400–900 nm with a spectral resolution of about 1.5 nm. Radiometer 1, equipped with a 25° field-of-view optical fiber was pointed downward to measure the upwelling radiance of the crop (L_λ^{crop}). The position of the radiometer above the canopy was kept constant throughout the growing season (i.e., around 5.4 m), yielding a sampling area with a diameter of around 5 m. Radiometer 2, equipped with an optical fiber and cosine diffuser (yielding a hemispherical field of view), was pointed upward to simultaneously measure incident irradiance (E_λ^{inc}). The intercalibration of the radiometers was accomplished, in order to match their transfer functions,

by measuring the upwelling radiance (L_λ^{cal}) of a white Spectralon (Labshere, Inc., North Sutton, New Hampshire) reflectance standard simultaneously with incident irradiance (E_λ^{cal}). To mitigate the impact of solar elevation on radiometer intercalibration, the anisotropic reflectance from the calibration target was corrected in accord with *Jackson et al.* [1992]. Percent reflectance (R_λ) was computed as:

$$R_\lambda = \left(L_\lambda^{crop}/E_\lambda^{inc}\right) \times \left(E_\lambda^{cal}/L_\lambda^{cal}\right) \times 100 \times R_\lambda^{cal} \qquad (6)$$

where L_λ^{crop} and E_λ^{inc} are the outputs of the downward (upwelling radiance of crop) and upward (incident irradiance) pointing instruments, respectively; R_λ^{cal} is the reflectance of the Spectralon panel linearly interpolated to match the band centers of each radiometer; L_λ^{cal} is the output of the downward looking instrument when measuring the upwelling irradiance of the Spectralon panel; E_λ^{cal} is the output of the upward pointing instrument measuring incident irradiance during the time of calibration by means of the Spectralon panel. L_λ^{crop}, E_λ^{inc}, L_λ^{cal} and E_λ^{cal} are in digital numbers per second, corrected for the instruments' dark current. Sensors were configured to take fifteen simultaneous upwelling radiance and downwelling irradiance measurements, which were internally averaged and stored as a single data file. Radiometric data were collected close to solar noon (between 1100 and 1500 LT), when changes in solar zenith angle were minimal. The two radiometers were intercalibrated immediately before and immediately after measurements in each site.

[20] Our ultimate goal was to eliminate the need to use a calibration panel after each reflectance measurement and to avoid errors due to atmospheric variability during data collection. The use of two intercalibrated hyperspectral radiometers allows simultaneous measurement of downwelling irradiance and upwelling target radiance. Therefore it is possible to compute the radiance reflectance of a target during times when the incident radiation is highly variable. Such situations are difficult, if not impossible, when using one radiometer and measuring a reference panel after each target scan. The dual-fiber approach results in rapid measurement and minimal error due to variation in irradiation condition [*Rundquist et al.*, 2004]. A critical issue with regard to the dual-fiber approach is that the transfer functions (the ratio of the optical signal at the output of the system (in digital numbers) to the optical signal that is launched into the system) of both radiometers must be identical. We tested our Ocean Optics instruments under laboratory and field conditions; over a 4-hour period the standard deviations of the ratio of the two transfer functions did not exceed 0.004 (details given by *Dall'Olmo and Gitelson* [2005]).

[21] Spectral reflectance measurements at canopy level were carried out from June until October in 2001 growing season (18 measurement campaigns), and from May until October in 2002 and 2003 (31 and 34 measurement campaigns in 2002 and 2003, respectively). Reflectance measurements were made within an area of ~0.8 ha for each of the three sites. A total of 36 points within these areas were sampled per measurement date and site, and the median was calculated. Since eddy covariance measurements represent GPP of the entire site, while reflectance data were sampled

Table 2. T-Test Values and Their Respective P-Values for the Comparison of Means of the Index ($R_{NIR}/R_{Red-edge} - 1$) Calculated From Reflectance Data Acquired by the AISA System During the 2002 Growing Season, Within the Reflectance Sampling Areas and the Entire Sites

Date	T-Test	P-Value
Irrigated Maize (Site 1)		
21 June 2002	0.757	0.462[a]
27 June 2002	0.913	0.377
12 July 2002	1.299	0.215
15 July 2002	2.012	0.06
7 September 2002	1.159	0.266
17 September 2002	1.628	0.126
Irrigated Soybean (Site 2)		
21 June 2002	0.283	0.781
27 June 2002	0.185	0.856
12 July 2002	0.556	0.587
15 July 2002	0.615	0.549
7 September 2002	−0.283	0.781
17 September 2002	−0.709	0.490
Rainfed Soybean (Site 3)		
21 June 2002	−0.451	0.671[a]
27 June 2002	0.059	0.955[a]
12 July 2002	−0.211	0.836
15 July 2002	−1.846	0.092
7 September 2002	−3.222	0.008[b]
17 September 2002	−2.081	0.083[a]

[a]Two-sample T-test assuming unequal variances.
[b]Statistically significant difference.

in specific areas of the site, a test of site homogeneity was needed to assess if the reflectance sampling areas were representative of the entire site. For this, we used imagery acquired during the 2002 growing season (on 21 June, 27
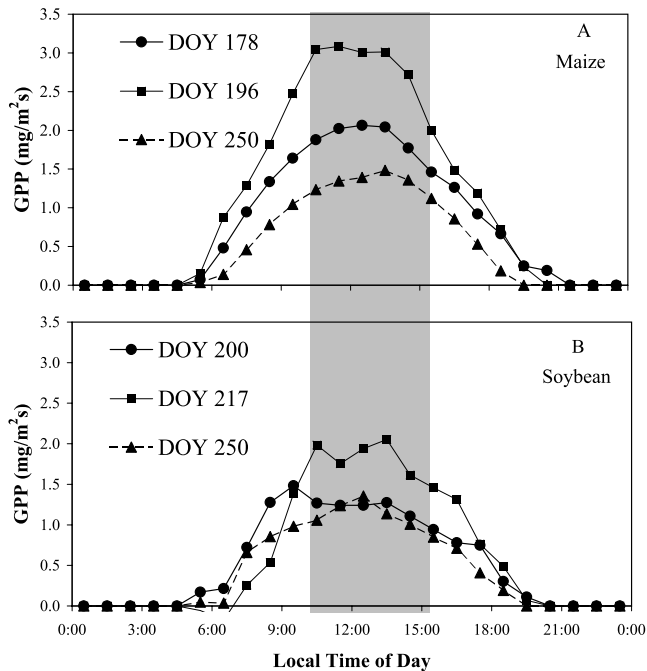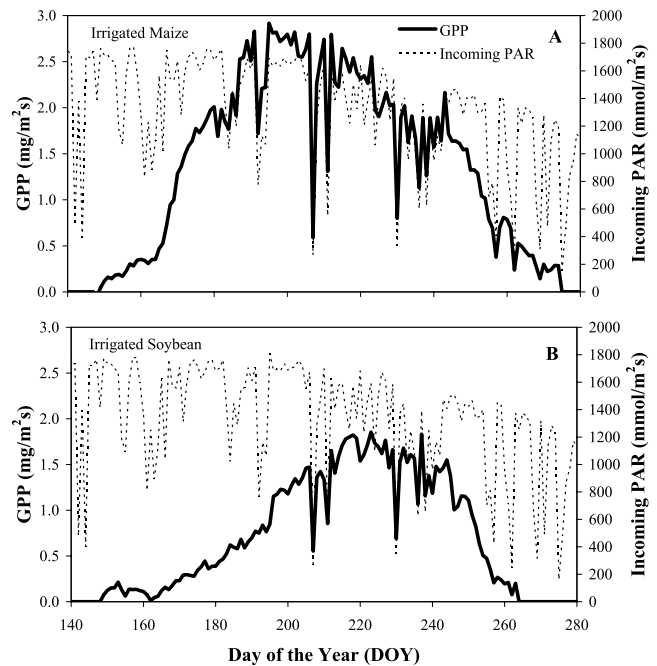

Figure 2. Temporal progression of measured midday GPP (solid line) and incident PAR (dotted line) in irrigated (a) maize and (b) soybean sites during the 2002 growing season.

June, 12 July, 15 July, 7 September, and 17 September) by an AISA (Oulu, Finland) hyperspectral imaging system, programmed to acquire 35 spectral bands between 400 and 900 nm. Measurements were carried out from an altitude of ∼1000 m, providing a spatial resolution ∼3 m/pixel. Green LAI was calculated as $[(R_{840-870}/R_{700-710}) - 1]$ [*Gitelson et al.*, 2003b] for each of these images, and the values from the entire sites and from the spectral reflectance sampling areas were compared on a per site and date basis, using a two-sample T-test, after checking for variance homogeneity. Site average values of this index that are significantly different from those of the spectral reflectance sampling areas would mean that the spectral sampling areas are not representative of the sites, and thus an overestimation or underestimation of the remote GPP estimate might occur. With the exception of site 3 on 7 September 2002 (which showed a statistically significant underestimation of the green LAI in the reflectance sampling area, as compared to the entire site), no statistically significant differences were obtained (Table 2). Therefore the spectral reflectances for the sampled areas were representative of the entire site.

2.7. Calibration and Validation of the Models

[22] Canopy spectral reflectance data were used to establish a new approach to assess remotely the GPP of crops. Daily midday GPP values (measured between 1000 and 1500 LT) were used in the analysis (Figure 1). This approach was tested by means of regression analysis. Models between remotely sensed reflectances and GPP were developed and calibrated for irrigated and rainfed maize using data acquired during the 2001 and 2002 growing seasons, 78 samples, and irrigated and rainfed soybean using data acquired in 2002, 58 samples

Figure 1. Diurnal variation of GPP in (a) maize and (b) soybean for selected days of the year (DOY) during the growing season. The midday GPP used in this study is highlighted.
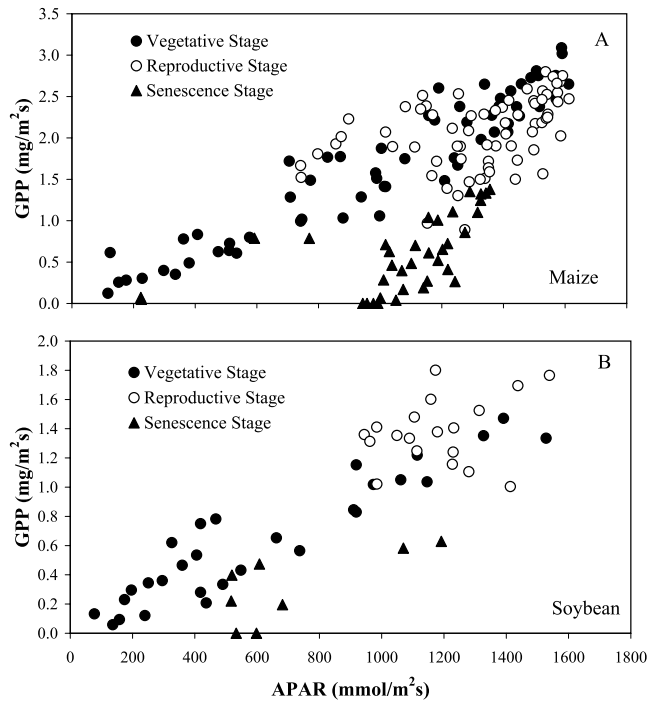
Figure 3. Midday GPP plotted versus absorbed photosynthetically active radiation (APAR) calculated as APAR = fAPAR × PAR for (a) irrigated and two rainfed maize in 2001–2002 (Table 1) and (b) irrigated and rainfed soybean site in 2002.

(Table 1). The RMSE of GPP estimation by the developed models for each species was obtained. Then calibrated models for GPP estimation were inverted and validated for irrigated and rainfed maize using spectral reflectance and GPP data collected during the growing season of 2003, (97 samples, Table 1). To provide the context for the approach described in this study, other existing models for GPP assessment were also tested in order to evaluate their accuracy of GPP estimation and compare them to the models developed in this study.

3. Results and Discussion

[23] Temporal progressions of midday GPP as well as incident PAR during the growing season are shown for irrigated maize (Figure 2a) and irrigated soybean (Figure 2b). The temporal variability of GPP along the growing season contains two types of variation: a low frequency variation (day-to-day), which relates to both phenological development and long-term stresses, and a high frequency variation (diurnal), which relates mostly to changes in radiation conditions but also to short-term stresses.

[24] To evaluate the assumption that a constant LUE holds for the crops studied, we analyzed the relationship between GPP and APAR calculated as the product of fAPAR and PAR and plotted versus GPP (Figure 3). For both maize and soybean, the behavior of GPP versus APAR was different at three distinctive phenological stages. Dur-
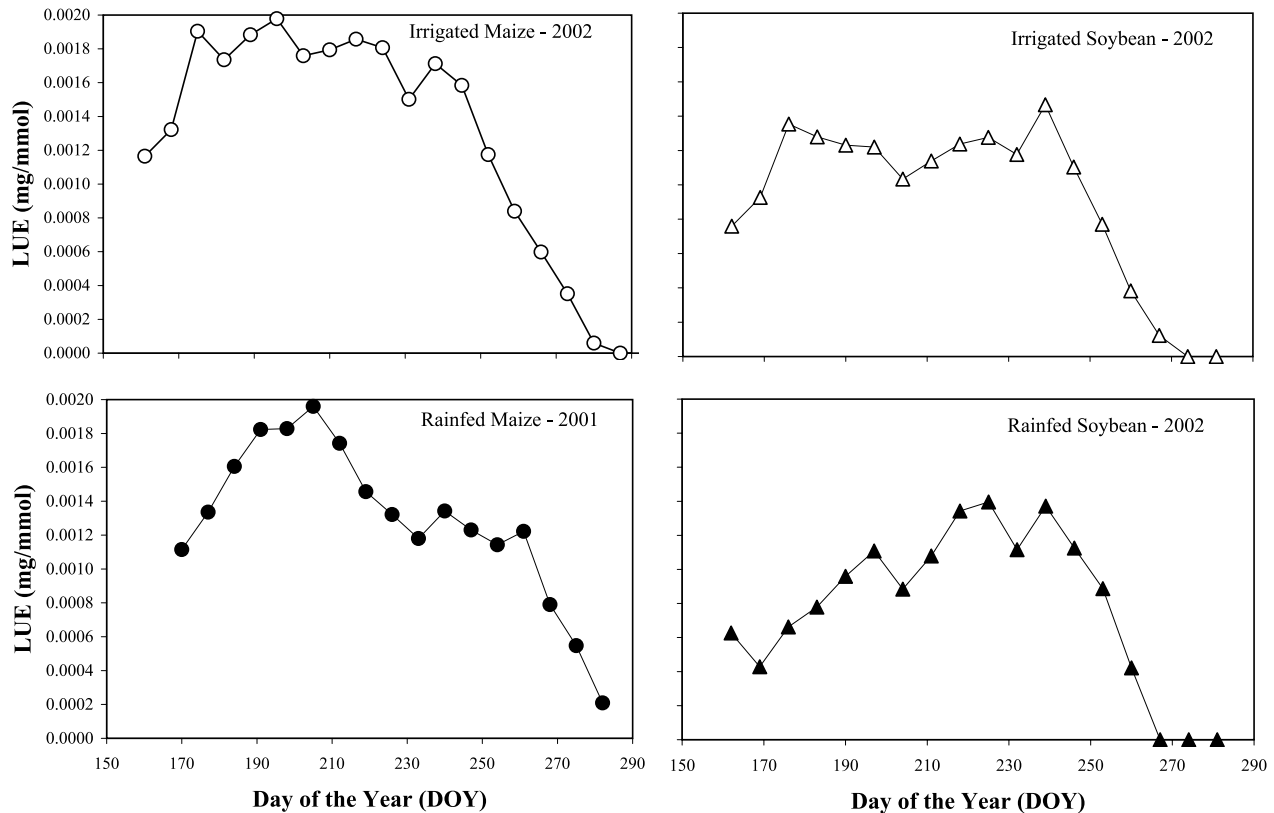

Figure 4. Temporal variability of canopy light use efficiency (LUE) of irrigated and rainfed maize and soybean. LUE is expressed as the ratio of weekly sums of midday (1000–1500 LT) GPP and absorbed PAR.
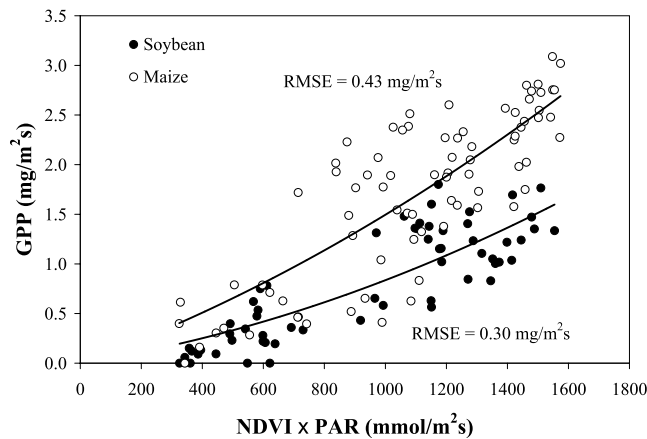
Figure 5. Midday GPP plotted versus the NDVI × PAR for irrigated and rainfed maize in 2001–2002 (Table 1) and irrigated and rainfed soybean in 2002.

ing the vegetative stage, GPP was almost linearly related with APAR. In contrast, no clear relationship was observed during the reproductive stage. During senescence, the relationship between GPP and APAR was also close to linear, but with a much higher slope than that observed during the vegetative stage. Therefore, although there was a nearly linear relationship between GPP and APAR during some time periods, the nature of this relationship changes with the phenological stage of the crop, suggesting that LUE of the crops studied changes along the growing season.

[25] To further examine this matter, we calculated weekly LUE as: LUE = GPP/(fAPAR*PAR), and plotted it versus day of the year (DOY, Figure 4). LUE showed considerable variation during the growing season. During the vegetative stage it increased until reaching maximal values in the middle of the growing season (around 0.002 mg/mmol for maize and 0.0015 mg/mmol for soybean). During the reproductive stage, LUE of irrigated maize remained almost invariable for about 30 days and then declined sharply during senescence. In rainfed maize, a conspicuous decline of LUE can be seen in the middle of growing season that related to a period of moisture stress (see for details *Suyker et al.* [2005]). Then, in the reproductive stage LUE gradually decreased, and it dropped sharply during senescence. As in maize, LUE of irrigated soybean did not show a high variation during the middle of the growing season, while in rainfed soybean it increased gradually reaching maximum around DOY 240 and dropped conspicuously just after reaching maximal values.

[26] We also examined the relationship between GPP and the product of NDVI and PAR (Figure 5), i.e., the NDVI was used as a proxy of fAPAR [e.g., *Sellers et al.*, 1992; *Ruimy et al.*, 1994; *Running et al.*, 2000]. For both species there was large dispersion of points around the best fit function, which is reflected in the high RMSE values of GPP estimation: 0.43 mg/m²s for maize and 0.3 mg/m²s for soybean. These results show that in the crops studied LUE varied significantly during the growing season and this variation has to be taken into consideration in any algorithm for the remote estimation of GPP.

[27] To test the efficiency of PRI as a proxy of LUE in crops, we calculated a scaled PRI (as suggested by *Rahman et al.* [2004]) as sPRI = (1 + PRI)/2 and plotted GPP as a function of the product PAR × NDVI × sPRI (Figure 6). For both species, the parabolic relationships between GPP and PAR × NDVI × sPRI were slightly better than that between GPP and PAR × NDVI: for maize RMSE was 0.39 mg/m²s (versus 0.43 mg/m²s for PAR × NDVI) and for soybean RMSE was 0.29 mg/m²s (versus 0.30 mg/m²s for PAR × NDVI). However, no major improvement was observed. Our results showed the difficulty in using this index at a scale larger than the leaf. Similar results showing no relationships for PRI versus LUE at canopy level have been reported previously [*Carter*, 1998; *Gamon et al.*, 1992; *Methy*, 2000; *Barton and North*, 2001]. *Methy* [2000] suggested that it is due to a relatively small reflectance signal and significant confounding effects such as physiological and structural heterogeneity of leaves in the field of view of the radiometer and the possibly changing structure of the canopy. Thus sPRI cannot be used as a proxy of LUE in maize and soybean, and new approaches are needed to accurately estimate GPP in crops.

[28] Following Monteith's logic, GPP is a function of the amount of PAR absorbed by the canopy (APAR) and the capacity of the leaves to export or utilize the product of photosynthesis (i.e., LUE). The product of APAR and LUE depends on the amount and distribution of photosynthetic biomass, thus of chlorophyll content and leaf physiology [*Sellers et al.*, 1992]. Therefore both APAR and LUE are closely related to the amount of chlorophyll in the canopy. Low frequency (day-to-day) variation in GPP is associated with crop phenological stage and physiological status. It has been shown also that this low frequency variation in GPP is closely related to green LAI in maize [*Suyker et al.*, 2004, 2005]. Our approach to estimate GPP remotely is based on the hypothesis that total canopy chlorophyll content (total Chl) in crops relates closely to the low frequency variation of GPP.

[29] To test this hypothesis, we calculated total Chl content in both crops and plotted the relationship between measured GPP and the product of PAR and total Chl
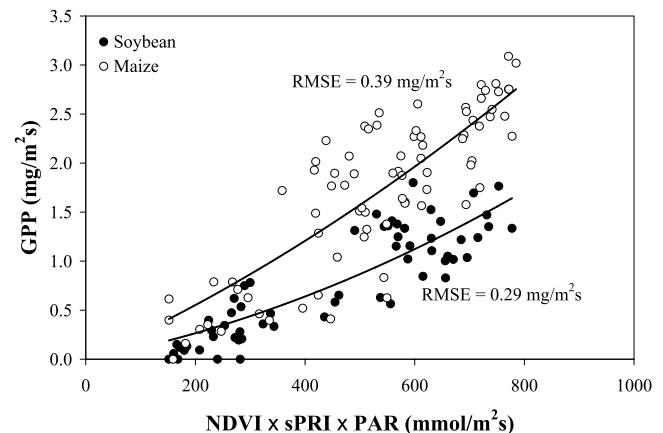

Figure 6. Midday GPP plotted versus the NDVI × sPRI × PAR for irrigated and rainfed maize in 2001–2002 (Table 1) and irrigated and rainfed soybean in 2002.
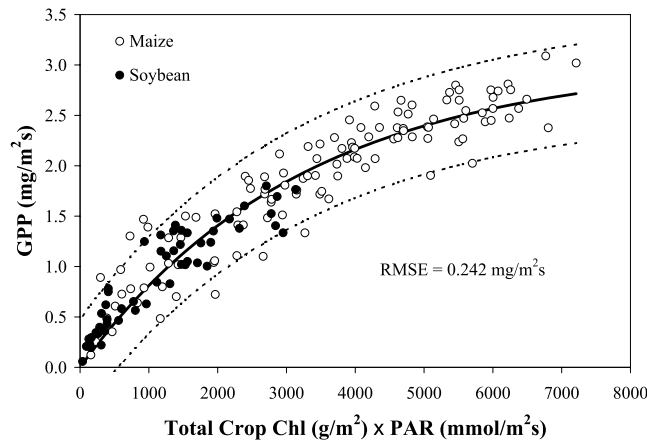
Figure 7. Midday GPP versus the product of PAR and total chlorophyll content in the irrigated and rainfed maize and soybean crops in 2001–2003 (Table 1).

(Figure 7). The best fit function for this relationship was $GPP = 3.04(1 - e^{-0.0003Chl \times PAR})$. The product of total Chl and PAR explained more than 98% of GPP variation in both irrigated and rainfed maize and soybean. Thus a procedure for assessing remotely GPP of crops may be implemented through the estimation of total canopy chlorophyll content.

[30] Changes in leaf Chl content induce large differences in canopy reflectance. However, these changes are masked and/or confounded by other factors (e.g., canopy architecture, Chl distribution within the canopy, LAI, soil background) that also affect canopy reflectance. Therefore remote Chl retrieval at canopy level is complicated and challenging. Recently, a conceptual model of the form $[R(\lambda_1)^{-1} - R(\lambda_2)^{-1}] \times R(\lambda_3)$, where $R(\lambda)$ is reflectance in three spectral bands (λ_1, λ_2 and λ_3), has been developed for pigment retrieval from reflectance spectra [*Gitelson et al.*, 2001, 2002, 2003a]. To assess Chl content in crops, this model was spectrally tuned to find the optimal positions of λ_1, λ_2 and λ_3, in accord with the optical properties of the crops. Optimal positions of spectral bands for the remote estimation of total Chl content in maize and soybean canopies were found in either the green (540–560 nm) or the red edge (700–730 nm) ranges for λ_1, and in the near infrared range (beyond 750 nm) for $\lambda_2 = \lambda_3$ [*Gitelson et al.*, 2005]. Taking into account that the product (total Chl) × PAR is closely related to GPP (Figure 7), we hypothesized that:

$$GPP \propto PAR \times \left(R_{green}^{-1} - R_{NIR}^{-1} \right) \times R_{NIR} = \left(R_{NIR}/R_{green} - 1 \right) \times PAR$$

(7)

$$GPP \propto PAR \times \left(R_{red\ edge}^{-1} - R_{NIR}^{-1} \right) \times R_{NIR}$$
$$= \left(R_{NIR}/R_{red\ edge} - 1 \right) \times PAR$$

(8)

The approach was tested and the models were calibrated for irrigated and rainfed maize using data from the 2001

through 2002 growing seasons and irrigated and rainfed soybean in 2002 (Table 1). Reflectance in the green (545–565 nm) and NIR (840–870 nm) discrete bands of the MODIS system, and the red edge (703.75–713.75 nm) and NIR (750–757.5 nm) bands of the MERIS system were simulated and used in the analyses. Both models were closely related to GPP in maize and soybean (Figure 8). RMSE of GPP estimation by the model ($R_{NIR}/R_{green} - 1$) was 0.3 mg/m^{2}s in maize (GPP from 0 to 3.089 mg/m^{2}s) and 0.2 mg/m^{2}s in soybean (GPP from 0 to 1.8 mg/m^{2}s). The precision of the model ($R_{NIR}/R_{red\ edge} - 1$) was higher: RMSE of GPP estimation was 0.27 mg/m^{2}s in maize and 0.15 mg/m^{2}s in soybean. Both models provided a more precise estimation of GPP than NDVI × PAR and NDVI × sPRI × PAR (Table 3); RMSE of GPP estimation by developed models (equations (7) and (8)) was at least 43% lower than that by NDVI × PAR.

[31] It is important to note that both models constitute a measure of total Chl content in crops. The coefficient of determination of the linear relationships ($R_{NIR}/R_{red\ edge} - 1$) versus total Chl and ($R_{NIR}/R_{green} - 1$) versus total Chl was 0.92 for maize and 0.94 for soybean [*Gitelson et al.*, 2005] while relationships between GPP and models (equations (7) and (8)) were non linear (Figure 8) with larger scattering of points from best fit functions. This is understandable,
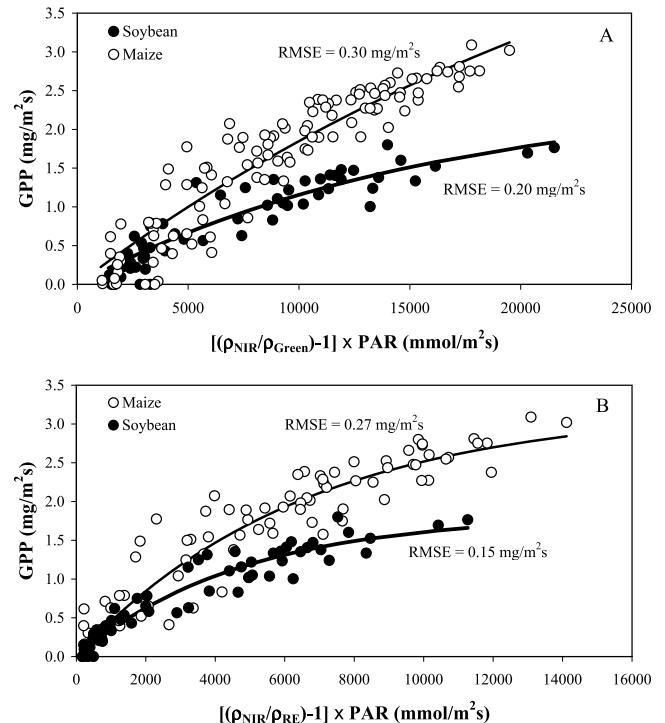

Figure 8. Relationships between midday GPP and (a) $[(R_{NIR}/R_{green}) - 1] \times PAR$ and (b) $[(R_{NIR}/R_{red\ edge}) - 1] \times PAR$ for irrigated and rainfed maize in 2001–2002 and soybean in 2002 (Table 1). Reflectance in the green (545–565 nm) and NIR (840–870 nm) discrete bands of the MODIS system and the red edge (703.75–713.75 nm) and NIR (750–757.5 nm) bands of the MERIS system were simulated and used in the analyses.

Table 3. Calibration of the Models for GPP Estimation for Irrigated and Rainfed Maize in 2001–2002 (Table 1) and Irrigated and Rainfed Soybean in 2002[a]

	Maize		Soybean	
Model	Equation	RMSE	Equation	RMSE
x = NDVI	$GPP = 6e^{-7}x^2 + 0.0007x$	0.43	$GPP = 3e^{-7}x^2 + 0.0005x$	0.30
x = NDVI × PRI	$GPP = 2e^{-6}x^2 + 0.0017x$	0.39	$GPP = 1e^{-6}x^2 + 0.0011x$	0.29
x = equation (7)	$GPP = 6.6(1 - e^{-0.000032x})$	0.30	$GPP = 2.47(1 - e^{-0.000063x})$	0.20
x = equation (8)	$GPP = 3.21(1 - e^{-0.0002x})$	0.27	$GPP = 1.83(1 - e^{-0.0002x})$	0.15
x = equation (9)	$GPP = 0.0013x$	0.30	$GPP = 0.0013x$	0.30

[a]Midday GPP ranged from 0 to 3.1 mg/m^{2}s in maize and from 0 to 1.8 mg/m^{2}s in soybean. Root Mean Square Error (RMSE) of GPP estimation in mg/m^{2}s. Note that the calibration coefficients of both models (equations (7) and (8)) as well as NDVI × PAR and NDVI × sPRI × PAR remain species-specific (Figures 5, 6, and 8), while best fit function GPP versus $(R_{840-870}/R_{720-740} - 1) \times PAR$ (equation (9) and Figure 9) showed no statistically significant differences between maize and soybean.

considering that GPP is affected also by short-term environmental stresses. If these stresses affect canopy Chl content, the models (equations (7) and (8)) describe it quite accurately. If these short-term stresses do not affect Chl content, the models fail to detect them.

[32] In addition, GPP depends on the composition of incident irradiation (the ratio of diffuse to direct light). At a given incident light, the GPP in maize is around 40% higher during cloudy conditions [*Suyker et al.*, 2004]. Canopy reflectance also depends on atmospheric conditions. When a cloud obscures the sun, the proportion of incoming diffuse radiation increases relative to the incoming direct component; both the spectral quality and the angular distribution of the incoming radiation are affected. Canopy radiance is altered because of its angular anisotropy and, more importantly, because of the partial or complete removal of shadows formed by vegetation [e.g., *Colwell*, 1974]. Removing a 10% shadow component causes an increase in canopy reflectance of approximately 5% in the NIR and 8% in the green and the red edge; removing a 20% shadow component causes an increase in reflectance of 8% in the NIR and 15% in the green and red edge [*Gitelson et al.*, 2003c]. Thus the equations (7) and (8) underestimated GPP under cloudy conditions. Our reflectance measurements were carried out in both clear skies and in cloudy conditions. Therefore these factors affected the relationship GPP versus total canopy Chl and caused scattering of the points from the best fit function.

[33] As with canopy chlorophyll content estimation [*Gitelson et al.*, 2005], in the simulated discrete spectral ranges of MODIS and MERIS space-borne sensors, the calibration coefficients of both models (equations (7) and (8)) remained species-specific; slopes of the relationships "GPP versus model" for maize and soybean were significantly different (Figure 8). This behavior is understandable taking into account the contrasting canopy architectures and leaf structures of maize and soybean: (1) Soybean has a heliotropic leaf angle distribution while the leaf angle distribution in maize is hemispherical and (2) chlorophyll content in the adaxial surface of soybean leaves is higher than that in maize leaves, for the same total leaf Chl. Thus, for the same total Chl in the canopy, $R_{NIR}^{maize} < R_{NIR}^{soybean}$ and soybean has lower reflectance in the visible spectrum. This causes higher model values (thus higher GPP estimations) for soybean than for maize. Therefore we attempted to find a spectral range where the model is non-species-specific. As in the case of canopy chlorophyll content [*Gitelson et al.*,

2005], it has been found in the range 720–740 nm and 840–870 nm. The calibration parameters of the model:

$$GPP \propto PAR \times \left(R_{720-740}^{-1} - R_{840-870}^{-1}\right) \times R_{840-870}$$
$$= (R_{840-870}/R_{720-740} - 1) \times PAR \qquad (9)$$

showed no statistically significant differences between maize and soybean (Figure 9) and the model is able to estimate GPP in both species with a RMSE of less than 0.30 mg/m^{2}s, which is at least 30% lower than that provided by NDVI × PAR and NDVI × sPRI × PAR (Table 3). Thus this model can be used with a unique set of calibration coefficients under a mixed pixel scenario (including such contrasting canopy types as maize and soybean).

[34] While a statistically significant effect of crop type (i.e., maize and soybean) was found in the regression analyses performed (with the exception of equation (9)), no significant effect of water treatment (i.e., irrigated versus rainfed) was observed. This is an advantage of our approach; that is, our technique accurately estimates GPP independent of the type of treatment.
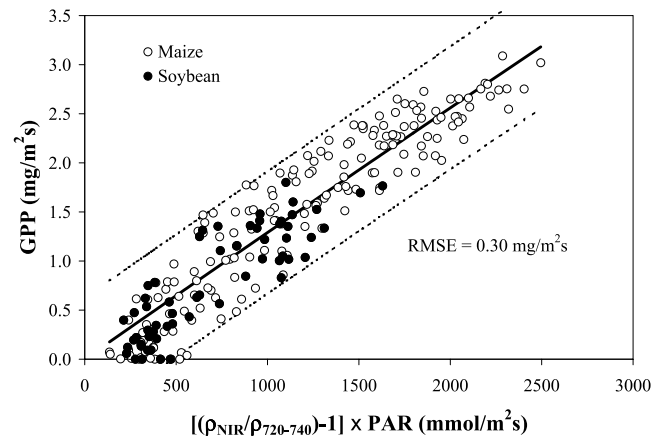

Figure 9. Midday GPP versus the model $(R_{NIR}/R_{720-740nm} - 1) \times PAR$ plotted for irrigated and rainfed maize in 2001–2002 (Table 1) and irrigated and rainfed soybean in 2002. The model is able to accurately estimate GPP in both maize and soybean. No statistically significant differences (p < 0.001) were obtained between regression parameters of maize and soybean.
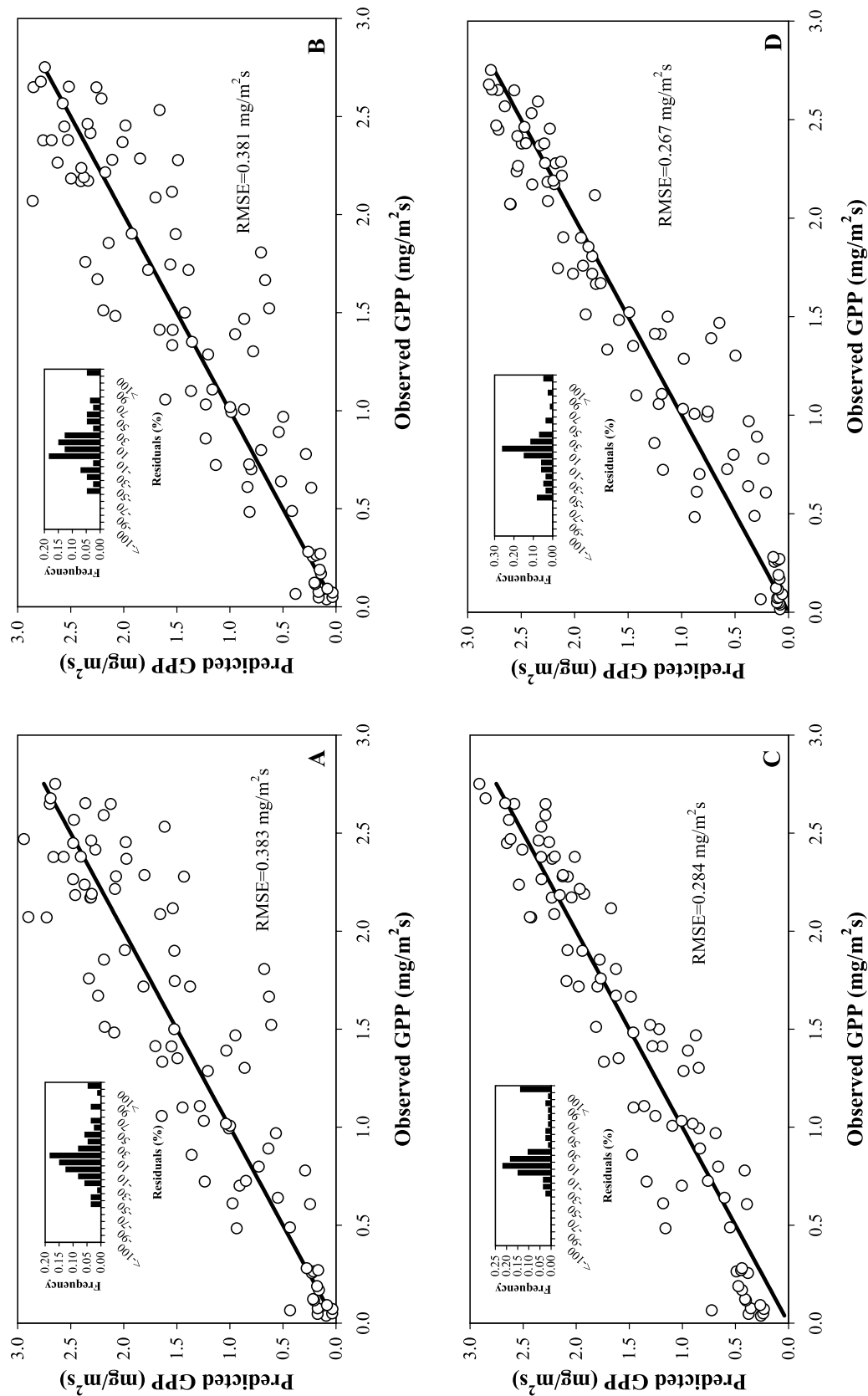
Figure 10. Validation of the models (a) NDVI × PAR, (b) NDVI × sPRI × PAR, (c) $[(R_{NIR}/R_{green}) - 1] \times$ PAR, and (d) $[(R_{NIR}/R_{red\ edge}) - 1] \times$ PAR for midday GPP prediction in irrigated and rainfed maize in 2003. Reflectance in the green (545–565 nm) and NIR (840–870 nm) discrete bands of the MODIS system and the red edge (703.75–713.75 nm) and NIR (750–757.5 nm) bands of the MERIS system were simulated and used in the analyses. Insets show the frequency distribution of the residuals from the 1-to-1 line (expressed as a percent).
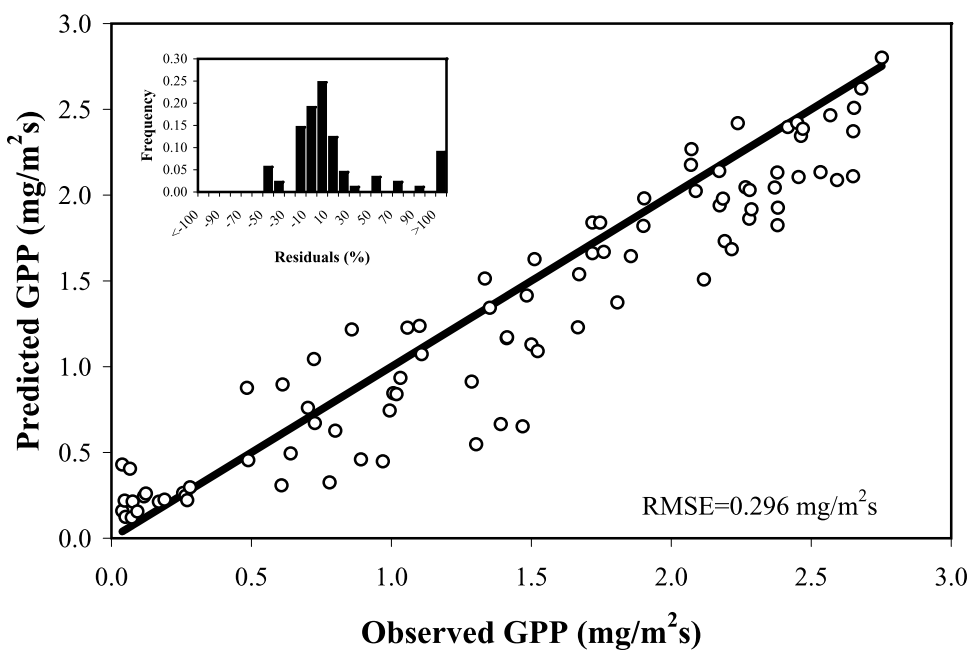
Figure 11. Validation of the model $[(R_{NIR}/R_{720-740}) - 1] \times PAR$ for midday GPP prediction in irrigated and rainfed maize in 2003. This model showed no significant difference in the coefficients for maize and soybean. Inset shows the frequency distribution of the residuals from the 1-to-1 line (expressed as a percent).

[35] Validation of the developed models (equations (7)–(9)) as well as NDVI × PAR and NDVI × sPRI × PAR for GPP prediction in maize was performed using an independent data set obtained in 2003 (97 samples, two irrigated sites and one rainfed site: Table 1). These data were used to predict GPP in maize using the models calibrated with data obtained in 2001 and 2002 (Table 3). Then, the predicted GPP values were compared with those actually measured in the 2003 growing season and the results of the comparison are shown in Figures 10 and 11. As with model calibration (Table 3), the model ($R_{NIR}/R_{red\ edge} - 1$) was superior in predicting midday GPP, but all three developed models (equations (7), (8), and (9)) were much more accurate in the estimation of GPP in the whole range of its variation than either the NDVI × PAR or the NDVI × sPRI × PAR.

4. Conclusions

[36] Chlorophyll content in irrigated and rainfed maize and soybean is closely related to midday gross primary production. A conceptual model, originally developed for pigment concentration retrieval in leaves and spectrally tuned for the remote estimation of chlorophyll content in crops [*Gitelson et al.*, 2005], was successfully applied for the retrieval of midday gross primary production in irrigated and rainfed soybean, at field level. This new technique is solely based on remotely sensed data, and provides a robust estimation of midday gross primary production in crops.

[37] Given the substantial improvement in the accuracy of midday gross primary production estimation by the models developed in this study, as compared to the currently used methods, it is worthwhile to fully explore the efficacy of these techniques over different crops, at different sites, and

through remote as opposed to proximal spectral sensors. Further validation of this technique over other crops and vegetation types is required using the green and NIR bands of satellite-based systems such as MODIS, Landsat TM and ETM, and Hyperion (on board EO-1 satellite) as well as the red-edge and NIR bands of satellite systems such as MERIS and Hyperion. With further validation (using data from already established FluxNet and SpecNet sites), this technique may be found useful in a variety of terrestrial ecosystems. The end result may be an inexpensive yet accurate tool for estimating midday GPP.

References

Ahl, D. E., S. T. Gower, D. S. Mackay, S. N. Burrows, J. M. Norman, and G. R. Diak (2004), Heterogeneity of light use efficiency in a northern Wisconsin forest: Implications for modeling net primary production with remote sensing, *Remote Sens. Environ.*, *93*, 168–178.

Asrar, G., M. Fuchs, E. T. Kanemasu, and J. H. Hatfield (1984), Estimating absorbed photosynthetic radiation and leaf area index from spectral reflectance in wheat, *Agron. J.*, *76*, 300–306.

Asrar, G., R. B. Myneni, and B. J. Choudhury (1992), Spatial heterogeneity in vegetation canopies and remote sensing of absorbed photosynthetically active radiation: A modeling study, *Remote Sens. Environ.*, *41*, 85–103.

Baldocchi, D. D. (2003), Assessing the eddy covariance technique for evaluating carbon dioxide exchange rates of ecosystems: Past, present and future, *Global Change Biol.*, *9*, 479–492.

Barford, C. C., S. C. Wofsy, M. L. Goulden, J. W. Munger, E. H. Pyle, S. P. Urbanski, L. Hutyra, S. R. Saleska, D. Fitzjarrald, and K. Moore (2001), Factors controlling long- and short-term sequestration of atmospheric CO_2 in a mid-latitude forest, *Science*, 294, 1688–1691.

Barton, C. V. M., and P. R. J. North (2001), Remote sensing of canopy light use efficiency using the photochemical reflectance index. Model and sensitivity analysis, *Remote Sens. Environ.*, 78, 264–273.

Biscoe, P. V., R. K. Scott, and J. L. Monteith (1975), Barley and its environment. III. Carbon budget of the stand, *J. Appl. Ecol.*, 12, 269–291.

Box, E. O. (1978), Geographical dimensions of terrestrial net and gross primary productivity, *Radiat. Environ. Biophys.*, 15, 305–322.

Cao, M., and F. I. Woodward (1998), Dynamic responses of terrestrial ecosystem carbon cycling to global climate change, *Nature*, 393, 249–252.

Carter, G. A. (1998), Reflectance wavebands and indices for remote estimation of photosynthesis and stomatal concuctance in pine canopies, *Remote Sens. Environ.*, 63, 61–72.

Colwell, J. E. (1974), Vegetation canopy reflectance, *Remote Sens. Environ.*, 3, 175–183.

Dall'Olmo, G., and A. A. Gitelson (2005), Effect of bio-optical parameter variability on the remote estimation of chlorophyll-a concentration in turbid productive waters: Experimental results, *Appl. Opt.*, 44, 412–422.

Dawson, T. P., P. R. J. North, S. E. Plummer, and P. J. Curran (2003), Forest ecosystem chlorophyll content: Implications for remotely sensed estimates of net primary productivity, *Int. J. Remote Sens.*, 24, 611–617.

Dixon, R. K., S. Brown, R. A. Houghton, A. M. Solomon, M. C. Trexlerm, and J. Wisniewski (1994), Carbon pools and flux of global forest ecosystems, *Science*, 263, 185–190.

Falge, E., et al. (2002), Seasonality of ecosystem respiration and gross primary production as derived from FLUXNET measurements, *Agric. For. Meteorol.*, 113, 53–74.

Flanagan, L. B., L. A. Wever, and P. J. Carlson (2002), Seasonal and interannual variation in carbon dioxide exchange and carbon balance in a northern temperate grassland, *Global Change Biol.*, 8, 599–615.

Gamon, J. A., J. Penuelas, and C. B. Field (1992), A narrow waveband spectral index that tracks diurnal changes in photosynthetic efficiency, *Remote Sens. Environ.*, 4, 35–44.

Gilmanov, T. G., S. B. Verma, P. Sims, T. P. Meyers, J. A. Bradford, G. G. Burba, and A. E. Suyker (2003), Gross-primary production of four Southern Plains ecosystems estimated using long-term CO_2 flux tower measurements, *Global Biogeochem. Cycles*, 17(2), 1071, doi:10.1029/2002GB002023.

Gitelson, A. A., M. N. Merzlyak, and O. B. Chivkunova (2001), Optical properties and non-destructive estimation of anthocyanin content in plant leaves, *Photochem. Photobiol.*, 74, 38–45.

Gitelson, A. A., Y. Zur, O. B. Chivkunova, and M. N. Merzlyak (2002), Assessing carotenoid content in plant leaves with reflectance spectroscopy, *Photochem. Photobiol.*, 75, 272–281.

Gitelson, A. A., U. Gritz, and M. N. Merzlyak (2003a), Relationships between leaf chlorophyll content and spectral reflectance and algorithms for non-destructive chlorophyll assessment in higher plant leaves, *J. Plant Physiol.*, 160, 271–282.

Gitelson, A. A., A. Viña, T. J. Arkebauer, D. C. Rundquist, G. Keydan, and B. Leavitt (2003b), Remote estimation of leaf area index and green leaf biomass in maize canopies, *Geophys. Res. Lett.*, 30(5), 1248, doi:10.1029/2002GL016450.

Gitelson, A. A., S. B. Verma, A. Viña, D. C. Rundquist, G. Keydan, B. Leavitt, T. J. Arkebauer, G. G. Burba, and A. Suyker (2003c), Novel technique for remote estimation of CO_2 flux in maize, *Geophys. Res. Lett.*, 30(9), 1486, doi:10.1029/2002GL016543.

Gitelson, A. A., A. Viña, V. Ciganda, D. C. Rundquist, and T. J. Arkebauer (2005), Remote estimation of canopy chlorophyll content in crops, *Geophys. Res. Lett.*, 32, L08403, doi:10.1029/2005GL022688.

Goward, S. N., and K. F. Huemmrich (1992), Vegetation canopy PAR absorptance and the normalized difference vegetation index: An assessment using the SAIL model, *Remote Sens. Environ.*, 39, 119–140.

Jackson, R. D., T. R. Clarke, and M. S. Moran (1992), Bidirectional calibration results for 11 Spectralon and 16 $BaSO_4$ reference reflectance panels, *Remote Sens. Environ.*, 40, 231–239.

Jarvis, P. G., and J. W. Leverenz (1983), Productivity of temperature, deciduous and evergreen forests, in *Encyclopedia of Plant Physiology, New Series*, vol. 12d, edited by O. L. Lange et al., pp. 233–280, Springer, New York.

Knipling, E. B. (1970), Physical and physiological bases for the reflectance of visible and near-infrared radiation from vegetation, *Remote Sens. Environ.*, 1, 155–159.

Lieth, H. (1975), Historical survey of primary productivity research, in *Primary Productivity of the Biosphere, Ecological Studies*, vol. 14, edited by H. Lieth and R. H. Whittaker, pp. 7–16, Springer, New York.

Massman, W. J. (1991), The attenuation of concentration fluctuations in turbulent flow in a tube, *J. Geophys. Res.*, 96, 15,269–15,273.

Methy, M. (2000), Analysis of photosynthetic activity at the leaf and canopy levels from reflectance measurements: A case study, *Photosynthetica*, 38, 505–515.

Minasny, B., and A. B. McBratney (2003), FuzME version 3.0, Aust. Cent. for Precis. Agric., Univ. of Sydney, Sydney, N. S. W., Australia. (Available at http://www.usyd.edu.au/su/agric/acpa)

Monteith, J. L. (1972), Solar radiation and productivity in tropical ecosystems, *J. Appl. Ecol.*, 9, 744–766.

Monteith, J. L. (1977), Climate and the efficiency of crop production in Britain, *Philos. Trans. R. Soc. London*, 281, 277–294.

Moore, C. J. (1986), Frequency response correction for eddy correlation systems, *Boundary Layer Meteorol.*, 37, 17–35.

Myneni, R. B., C. D. Keeling, C. J. Tucker, G. Asrar, and R. R. Nemani (1997), Increased plant growth in the northern high latitudes from 1981 to 1991, *Nature*, 386, 698–702.

Myneni, R. B., J. Dong, C. J. Tucker, R. K. Kaufmann, P. E. Kuppi, J. Liski, L. Zhou, V. Alexyev, and M. K. Hughes (2001), A large carbon sink in the woody biomass of Northern forests, *Proc. Natl. Acad. Sci. U. S. A.*, 98, 14,784–14,789.

Nichol, C. J., K. F. Huemmrich, T. A. Black, P. G. Jarvis, C. L. Walthall, J. Grace, and F. G. Hall (2000), Remote sensing of photosynthetic-light-use efficiency of boreal forest, *Agric. For. Meteorol.*, 101, 131–142.

Nichol, C. J., J. Lloyd, O. Shibistova, A. Arneth, C. Roser, A. Knohl, S. Matsubara, and J. Grace (2002), Remote sensing of photosynthetic-light-use efficiency of a Siberian boreal forest, *Tellus, Ser. B*, 54, 677–687.

Rahman, A. F., V. D. Cordova, J. A. Gamon, H. P. Schmid, and D. A. Sims (2004), Potential of MODIS ocean bands for estimating CO_2 flux from terrestrial vegetation: A novel approach, *Geophys. Res. Lett.*, 31, L10503, doi:10.1029/2004GL019778.

Roujean, J. L., and F. M. Breon (1995), Estimating PAR absorbed by vegetation from bidirectional reflectance measurements, *Remote Sens. Environ.*, 51, 375–384.

Ruimy, A., B. Saugier, and G. Dedieu (1994), Methodology for the estimation of terrestrial net primary production from remotely sensed data, *J. Geophys. Res.*, 99, 5263–5283.

Ruimy, A. L., P. G. Jarvis, D. D. Baldocchi, and B. Saugier (1995), CO_2 fluxes over plant canopies and solar radiation: A review, *Adv. Ecol. Res.*, 26, 1–68.

Ruimy, A., L. Kergoat, and A. Bondeau (1999), Comparing global models of terrestrial net primary productivity (NPP): Analysis of differences in light absorption and light-use efficiency, *Global Change Biol.*, 5, 56–64.

Rundquist, D. C., R. Perk, B. Leavitt, G. P. Keydan, and A. A. Gitelson (2004), Collecting spectral data over cropland vegetation using machine-positioning versus hand-positioning of the sensor, *Comput. Electron. Agric.*, 43, 173–178.

Running, S. W., P. E. Thornton, R. Nemani, and J. M. Glassy (2000), Global terrestrial gross and net primary productivity from the Earth Observing System, in *Methods in Ecosystem Science*, edited by O. E. Sala et al., pp. 44–57, Springer, New York.

Running, S. W., R. R. Nemani, F. A. Heinsch, M. S. Zhao, M. Reeves, and H. Hashimoto (2004), A continuous satellite-derived measure of global terrestrial primary production, *Bioscience*, 54, 547–560.

Schimel, D. S. (1998), Climate change: The carbon equation, *Nature*, 393, 208–210.

Schuepp, P. H., M. Y. Leclerc, J. I. Macpherson, and R. L. Desjardins (1990), Footprint prediction of scalar fluxes from analytical solutions of the diffusion equation, *Boundary Layer Meteorol.*, 50, 355–373.

Sellers, P. J. (1985), Canopy reflectance, photosynthesis and transpiration, *Int. J. Remote Sens.*, 6, 1335–1372.

Sellers, P. J. (1987), Canopy reflectance, photosynthesis and transpiration II. The role of biophysics in the linearity of their independence, *Remote Sens. Environ.*, 21, 143–183.

Sellers, P. J., J. A. Berry, G. J. Collatz, C. B. Field, and F. G. Hall (1992), Canopy reflectance, photosynthesis and transpiration. III. A reanalysis using improved leaf models and a new canopy integration scheme, *Remote Sens. Environ.*, 42, 187–216.

Suyker, A. E., and S. B. Verma (1993), Eddy correlation measurements of CO_2 flux using a closed-path sensor: Theory and field tests against an open-path sensor, *Boundary Layer Meteorol.*, 64, 391–407.

Suyker, A. E., S. B. Verma, and G. G. Burba (2003), Interannual variability in net CO_2 exchange of a native tallgrass prairie, *Global Change Biol.*, 9, 1–11.

Suyker, A. E., S. B. Verma, G. G. Burba, T. J. Arkebauer, D. T. Walters, and K. G. Hubbard (2004), Growing season carbon dioxide exchange in irrigated and rainfed maize, *Agric. For. Meteorol.*, 124, 1–13.

Suyker, A. E., S. B. Verma, G. G. Burba, and T. J. Arkebauer (2005), Gross primary production and ecosystem respiration of irrigated maize and irrigated soybean during a growing season, *Agric. For. Meteorol.*, *131*, 180–190.

Turner, D. P., S. Urbanski, D. Bremer, S. C. Wofsy, T. Meyers, S. T. Gower, and M. Gregory (2003), A cross-biome comparison of daily light use efficiency for gross primary production, *Global Change Biol.*, *9*, 383–395.

Ustin, S. L., M. O. Smith, S. Jacquemoud, M. M. Verstraete, and Y. Govaerts (1998), GeoBotany: Vegetation mapping for earth sciences, in *Manual of Remote Sensing: Remote Sensing for the Earth Sciences*, 3rd ed., vol. 3, edited by A. N. Rencz, pp. 189–248, John Wiley, Hoboken, N. J.

Verma, S. B. (1990), Micrometeorological methods for measuring surface fluxes of mass and energy, *Remote Sens. Rev.*, *5*, 99–115.

Verma, S. B., et al. (2005), Annual carbon dioxide exchange in irrigated and rainfed maize-based agroecosystems, *Agric. For. Meteorol.*, *131*, 77–96.

Viña, A., and A. A. Gitelson (2005), New developments in the remote estimation of the fraction of absorbed photosynthetically active radiation in crops, *Geophys. Res. Lett.*, *32*, L17403, doi:10.1029/2005GL023647.

Viña, A., A. A. Gitelson, D. C. Rundquist, G. Keydan, B. Leavitt, and J. Schepers (2004), Monitoring maize (Zea mays L.) phenology with remote sensing, *Agron. J.*, *96*, 1139–1147.

Walter-Shea, E. A., J. Privett, D. Cornell, M. A. Mesarch, and C. J. Hays (1997), Relations between directional spectral vegetation indices and leaf area and absorbed radiation in alfalfa, *Remote Sens. Environ.*, *61*, 162–177.

Webb, E. K., G. I. Pearman, and R. Leuning (1980), Correction of flux measurements for density effects due to heat and water vapor transfer, *Q. J. R. Meteorol. Soc.*, *106*, 85–100.

Whittaker, R. H., and P. L. Marks (1975), Methods of assessing terrestrial productivity, in *Primary Productivity of the Biosphere, Ecological Studies*, vol. 14, edited by H. Lieth and R. H. Whittaker, pp. 55–118, Springer, New York.

Wofsy, S. C., and R. C. Harriss (2002), The North American Carbon Program (NACP): A report of the NACP committee of the U.S. Interagency Carbon Cycle Science Program, U.S. Global Change Res. Program, Washington, D. C.

Xu, L., and D. D. Baldocchi (2003), Seasonal variation in carbon dioxide exchange over a Mediterranean annual grassland in California, *Agric. For. Meteorol.*, *123*, 79–96.

Zarco-Tejada, P. J., J. R. Miller, G. H. Mohammed, T. L. Noland, and P. H. Sampson (2002), Vegetation stress detection through chlorophyll a+b estimation and fluorescence effects on hyperspectral imagery, *J. Environ. Qual.*, *31*, 1433–1441.

―――――――――――――

T. J. Arkebauer, Department of Agronomy and Horticulture, University of Nebraska, Lincoln, NE 68588-0517, USA.

G. G. Burba, Environmental Division, LI-COR Biosciences, Inc., P.O. Box 4425, Lincoln, NE 68504, USA.

V. Ciganda, A. A. Gitelson, G. Keydan, B. Leavitt, and D. C. Rundquist, Center for Advanced Land Management Information Technologies, University of Nebraska, 102 Nebraska Hall, Lincoln, NE 68588-0517, USA. (gitelson@calmit.unl.edu)

A. E. Suyker and S. B. Verma, School of Natural Resources, University of Nebraska, Lincoln, NE 68588-0517, USA.

A. Viña, Center for Systems Integration and Sustainability, Department of Fisheries and Wildlife, Michigan State University, 13 Natural Resources Building, East Lansing, MI 48824, USA.